# Chemistry on Surface-Confined Molecules: An Approach to Anchor Isolated Functional Units to Surfaces

**Arianna Friggeri,[†] Henk-Jan van Manen,[†] Tommaso Auletta,[†] Xue-Mei Li,[†] Szczepan Zapotoczny,[‡,§] Holger Schönherr,[‡,||] G. Julius Vancso,[‡] Jurriaan Huskens,*[,†] Frank C. J. M. van Veggel,*[,†] and David N. Reinhoudt*[,†]**

*Contribution from Supramolecular Chemistry and Technology, Materials Science and Technology of Polymers, and MESA+ Research Institute, University of Twente, P.O. Box 217, 7500 AE Enschede, The Netherlands*

*Received January 29, 2001*

**Abstract:** The synthesis of surface-confined, nanometer-sized dendrimers and Au nanoparticles was performed starting from single $Pd^{II}$ pincer adsorbate molecules (**10)** embedded as isolated species into 11-mercapto-1-undecanol and decanethiol self-assembled monolayers (SAMs) on gold. The coordination of monolayer-protected Au nanoclusters (MPCs) bearing phosphine moieties at the periphery (**13**), or dendritic wedges (**8**) having a phosphine group at the focal point, to SAMs containing individual $Pd^{II}$ pincer molecules was monitored by tapping mode atomic force microscopy (TM AFM). The individual $Pd^{II}$ pincer molecules embedded in the decanethiol SAM were visualized by their coordination to phosphine MPCs **13**; isolated objects with a height of 3.5 ± 0.7 nm were observed by TM AFM. Reaction of these embedded $Pd^{II}$ pincer molecules with the dendritic wedge **8** yielded individual molecules with a height of 4.3 ± 0.2 nm.

## Introduction

Nanometer-scale fabrication is a requirement for applications in the fields of, for example, future electronic devices,[1] high-density data storage,[2] drug delivery, and analytical chemistry.[3] One of the ultimate goals of nanofabrication/nanotechnology is computation by individual molecules.[4] To achieve single-molecule computation one must rely on the understanding and thus study of individual molecules. Single-molecule studies allow one to identify and examine individual members of a heterogeneous population, while ensemble studies only yield information on the average properties of a system.[5]

Single-molecule research began with biomolecules, in particular DNA, not only because they are the "building blocks of life" but also because of their large size, which facilitates their visualization.[6] The first imaging attempts, using scanning tunneling microscopy, date back to 1983.[7] In recent years, the development of optical tweezers has made the manipulation of single biomolecules possible,[8] and techniques such as scanning near-field optical microscopy (SNOM) and atomic force microscopy (AFM) can be used to study the physical,[9] dynamic,[10] and mechanical[11] properties of single molecules.

Nowadays, the dimensions of some synthetic molecular and supramolecular structures, for example dendrimers[12] and metal nanoparticles,[13] are in the same range as those of biological systems, and they have the desired dimensions of nano-electronic devices. Therefore, the "bottom-up" alternative, which consists of the controlled construction of complex structures of nanometer dimensions starting from the molecular level, is becoming an increasingly realistic tool for nanofabrication.[7]

* To whom correspondence should be addressed. Fax: +31 53 4894645. Telephone: +31 53 4892980. E-mail: smct@ct.utwente.nl.

[†] Supramolecular Chemistry and Technology, MESA+ Research Institute.

[‡] Materials Science and Technology of Polymers, MESA+ Research Institute.

[§] On leave from Jagiellonian University, Faculty of Chemistry, Ingardena 3, 30-060 Cracow, Poland.

[||] Current address: Stanford University, Department of Chemical Engineering, 381 North-South Mall, Stanford, CA, 94305, U.S.A.

(1) (a) Gittins, D. I.; Bethell, D.; Schiffrin, D. J.; Nichols, R. J. *Nature* **2000**, *408*, 67−69. (b) Collier, C. P.; Mattersteig, G.; Wong, E. W.; Luo, Y.; Beverly, K.; Sampaio, J.; Raymo, F. M.; Stoddart, J. F.; Heath, J. R. *Science* **2000**, *289*, 1172−1175. (c) Chen, J.; Reed, M. A.; Rawlett, A. M.; Tour, J. M. *Science* **1999**, *286*, 1550−1552.

(2) (a) Lutwyche, M. I.; Despont, M.; Drechsler, U.; Dürig, U.; Häberle, W.; Rothuizen, H.; Stutz, R.; Widmer, R.; Binnig, G. K.; Vettiger, P. *Appl. Phys. Lett.* **2000**, *77*, 3299−3301. (b) Mizutani, W.; Ishida, T.; Tokumoto, H. *Langmuir* **1998**, *14*, 7197−7202.

(3) Martin, C. R.; Mitchell, D. T. *Anal. Chem.* **1998**, May 1, 322 A-327 A.

(4) Ball, P. *Nature* **2000**, *406*, 118−120.

(5) Weiss, S. *Science* **1999**, *283*, 1676−1683.

(6) Service, R. F. *Science* **1999**, *283*, 1668−1669.

(7) Gimzewski, J. K.; Joachim, C. *Science* **1999**, *283*, 1683−1688.

(8) Mehta, A. D.; Rief, M.; Spudich, J. A.; Smith, D. A.; Simmons, R. M. *Science* **1999**, *283*, 1689−1695.

(9) Bayburt, T. H.; Carlson, J. W.; Sligar, S. G. *Langmuir* **2000**, *16*, 5993−5997.

(10) (a) Poirier, G. E. *Chem. Rev.* **1997**, *97*, 1117−1127. (b) Dunn, R. C. *Chem. Rev.* **1999**, *99*, 2891−2927. (c) Veerman, J. A.; Levi, S. A.; van Veggel, F. C. J. M.; Reinhoudt, D. N.; van Hulst, N. F. *J. Phys. Chem. A* **1999**, *103*, 11264−11270. (d) Takano, H.; Kenseth, J. R.; Wong, S.-S., O'Brien, J. C., Porter, M. D. *Chem. Rev.* **1999**, *99*, 2845−2890. (e) Ishii, Y., Yanagida, T. *Single Mol.* **2000**, *1*, 5−13.

(11) (a) Rief, M.; Oesterhelt, F.; Heymann, B.; Gaub, H. E. *Science* **1997**, *275*, 1295−1297. (b) Rief, M.; Gautel, M.; Oesterhelt, F.; Fernandez, J. M.; Gaub, H. E. *Science* **1997**, *276*, 1109−1112.

(12) For recent overviews of dendrimers, see: (a) Fischer, M.; Vögtle, F. *Angew. Chem., Int. Ed.* **1999**, *38*, 884−905. (b) Bosman, A. W.; Janssen, H. M.; Meijer, E. W. *Chem. Rev.* **1999**, *99*, 1665−1688. (c) Smith, D. K.; Diederich, F. *Chem. Eur. J.* **1998**, *4*, 1353−1361. (d) Newkome, G. R.; Moorefield, C. N.; Vögtle, F. *Dendritic Molecules: Concepts, Syntheses and Perspectives*; VCH: Weinheim, Germany, 1996.

(13) (a) Schmid, G.; Bäumle, M.; Geerkens, M.; Ingo, H.; Osemann, C.; Sawitowski, T. *Chem. Soc. Rev.* **1999**, *28*, 179−185. (b) Templeton, A. C.; Wuelfing, W. P.; Murray, R. W. *Acc. Chem. Res.* **2000**, *22*, 27−36.

10.1021/ja010257c CCC: $20.00 
Published on Web 06/09/2001

**Chart 1.** (a) Metallodendrimer Adsorbate **1**;[16] (b) Covalent Dendrimer Adsorbate **2**[17]

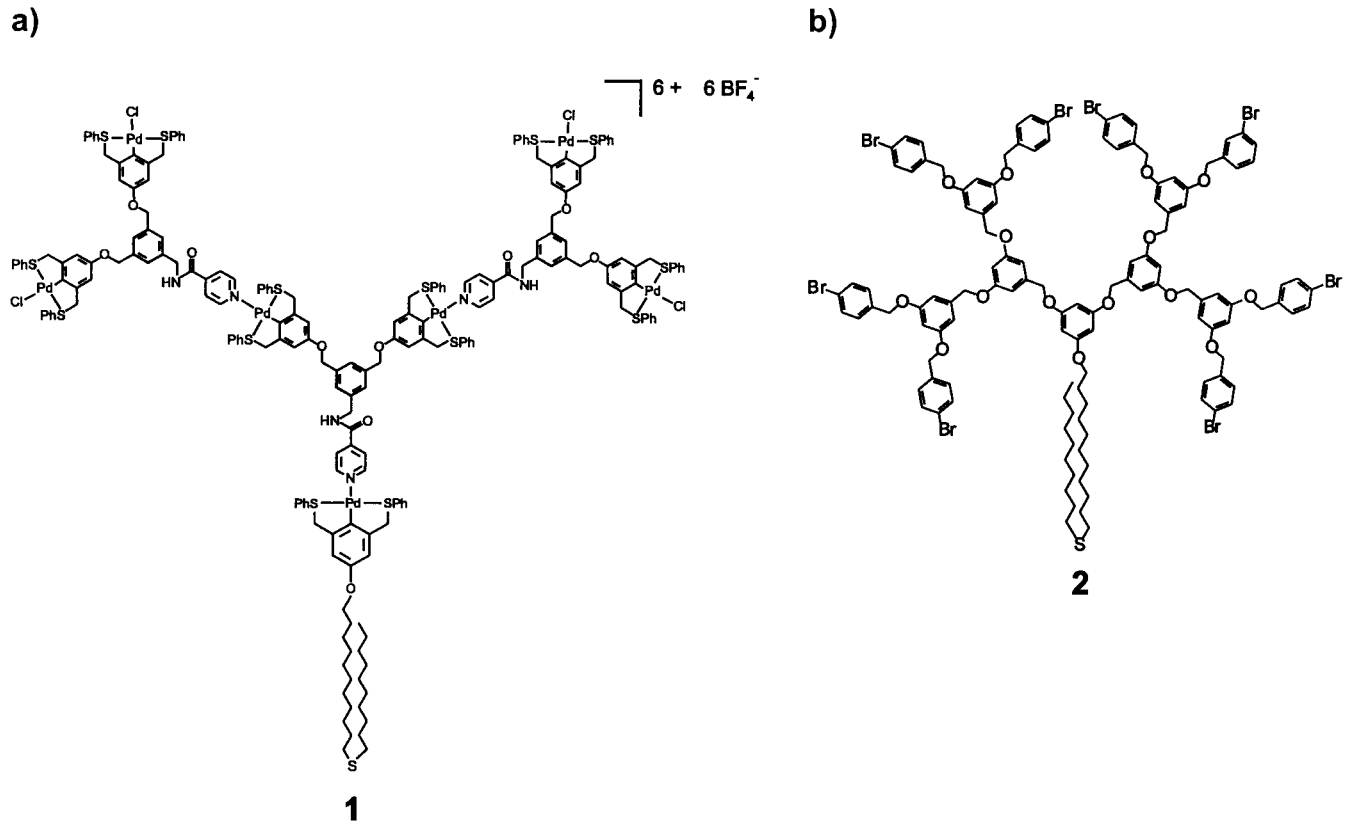


Self-assembled monolayers (SAMs) are useful starting platforms for the development of nanometer-scale devices,[14] since they are highly ordered and have uniform film thicknesses.[15] In our group we have developed metallodendrimer adsorbates such as **1** (Chart 1a) containing a dialkylsulfide moiety for anchorage to a gold substrate, and we have shown that these can be inserted into alkanethiol SAMs as single molecules.[16] The sulfide moiety was found to be essential for adsorption of the dendrimers to the gold surface. Furthermore, we have recently elucidated the insertion mechanism of individual molecules of the covalent dendrimer adsorbate **2** (Chart 1b) into 11-mercapto-1-undecanol SAMs.[17] AFM and electrochemistry data indicated that the dendrimer insertion is the rate-determining step of the process.

Further studies on the properties of single dendrimer molecules have recently been reported by several groups. Crooks and co-workers[18] have measured the height of G4 and G8 polyamidoamine (PAMAM) dendrimers on gold using TM AFM. Similarly, Tomalia and co-workers[19] have measured the molecular diameter and height of individual G5-G10 PAMAM dendrimers on mica, using TM AFM. However, AFM images of individual dendrimers smaller than G5 could not easily be obtained. De Schryver and co-workers[20] have used TM AFM to measure the height of G4 polyphenylene dendrimer molecules spin-coated on mica. Good agreement was found between the observed height and values calculated from molecular dynamics simulations. We have observed single metallodendrimer molecules containing a rhodamine B core using the SNOM technique.[10c]

Complementary contributions to the bottom-up approach originate from the use of metal or semiconductor nanoparticles, which can furthermore act as nanosized model systems for more complex molecular structures. Monolayer-protected nanoparticles have already shown to be versatile materials in several fields[21] due to their unique optical[22] and electronic properties[23] related to quantum size effects. Moreover, their straightforward synthesis allows introduction of a variety of terminal groups in the organic monolayer.[24]

(14) (a) Moav, T.; Hatzor, A.; Cohen, H.; Libman, J.; Rubinstein, I.; Shanzer, A. *Chem. Eur. J.* **1998**, *4*, 502−507. (b) Hatzor, A.; Moav, T.; Cohen, H.; Matlis, S.; Libman, J.; Vaskevich, A.; Shanzer, A.; Rubinstein, I. *J. Am. Chem. Soc.* **1998**, *120*, 13469−13477.

(15) (a) Ulman, A. *An Introduction to Ultrathin Organic Films from Langmuir−Blodgett to Self-Assembly*; Academic Press: San Diego, CA, 1991. (b) Ulman, A. *Chem. Rev.* **1996**, *96*, 1533−1554.

(16) Huisman, B.-H.; Schönherr, H.; Huck, W. T. S.; Friggeri, A.; van Manen, H.-J.; Menozzi, E.; Vancso, G. J.; van Veggel, F. C. J. M.; Reinhoudt, D. N. *Angew. Chem., Int. Ed.* **1999**, *38*, 2248−2251.

(17) Friggeri, A.; Schönherr, H.; van Manen, H.-J.; Huisman, B.-H.; Vancso, G. J.; Huskens, J.; van Veggel, F. C. J. M.; Reinhoudt, D. N *Langmuir* **2000**, *16*, 7757−7763.

(18) Hierlemann, A.; Campbell, J. K.; Baker, L. A.; Crooks, R. M.; Ricco, A. J. *J. Am. Chem. Soc.* **1998**, *120*, 5323−5324.

(19) Li, J.; Piehler, L. T.; Qin, D.; Baker Jr., J. R.; Tomalia, D. A. *Langmuir* **2000**, *16*, 5613−5616.

(20) Zhang, H.; Grim, P. C. M.; Foubert, P.; Vosch, T.; Vanoppen, P.; Wiesler, U.-M.; Berresheim, A. J.; Müllen, K.; De Schryver, F. C. *Langmuir* **2000**, *16*, 9009−9014.

(21) (a) Bartz, M.; Küther, J.; Seshadri, R.; Tremel, W.; *Angew. Chem., Int. Ed.* **1998**, *37*, 7, 2466−2468. (b) Labande, A.; Astruc, D. *Chem. Commun.* **2000**, 1007−1008. (c) Patolsky, F.; Ranjit, K. T.; Lichtenstein, A.; Willner, I. *Chem. Commun.* **2000**, 1025−1026.

(22) Thomas, K. G.; Kamat, P. V. *J. Am. Chem Soc.* **2000**, *122*, 2655−2656.

(23) (a) Elghanian, R.; Storhoff, J. J.; Mucic, R. C.; Letsinger, R. L.; Mirkin, C. A. *Science* **1997**, *277*, 1078−1081. (b) Schmid, G.; Bäumle, M.; Geerkens, M.; Heim, I.; Osemann, C.; Sawitowski, T. *Chem. Soc. Rev.* **1999**, *28*, 179−185. (c) Andres, R. P.; Bein, T.; Dorogi, M.; Feng, S.; Henderson, J. I.; Kubiak, C. P.; Mahoney, W.; Osifchin, R. G.; Reifenberger, R *Science* **1996**, *272*, 1323−1325.

(24) (a) Brust, M.; Walker, M.; Bethell, D.; Schiffrin, D. J.; Whyman, R. *J. Chem Soc., Chem Commun*. **1994**, 801−802. (b) Brust, M.; Fink, J.; Bethell, D.; Schiffrin, D. J.; Kiely, C. *J. Chem Soc., Chem Commun*. **1995**, 1655−1656. (c) Liu, J.; Alvarez, J.; Kaifer, A. E. *Adv. Mater.* **2000**, *12*, 1381−1383.

Although several publications regarding single-molecule imaging have appeared in the literature in the past few years[7−10,18−20] and coordination reactions have successfully been performed on SAMs on gold,[25] coordination chemistry on surface-immobilized, isolated molecules have, to the best of our knowledge, not been reported. In this article, the synthesis of isolated nanometer-sized objects starting from single molecules embedded in SAMs on gold is described. We first describe the coordination reactions onto isolated $Pd^{II}$ pincer adsorbate molecules in alkanethiol monolayers. Subsequently we show that individual $Pd^{II}$ pincer systems react with MPCs and dendritic molecules, leading to the spatial confinement of nanosized features. In both cases we present evidence that the process is indeed governed by metal−ligand coordination.

## Results and Discussion

**Synthesis of Phosphine-Derivatized, Monolayer-Protected Gold Clusters.** Au nanoparticles stabilized by a mixed monolayer of decanethiol and 11-mercapto-1-undecanol in a 4/1 ratio were prepared in a one-pot synthesis following the Brust method.[24a] $^1$H NMR spectroscopy ($CDCl_3$) showed that the percentage of the two thiols in the monolayer is the same as that in the solution from which the nanoparticles are formed (ca. 20 OH moieties per nanoparticle), indicating that the layer formation is under kinetic control. After purification of the product, the hydroxyl moieties were coupled with 4-(diphenylphosphino)benzoic acid in the presence of 1-(3-dimethylaminopropyl)-3-ethyl-carbodiimide hydrochloride (EDC) and 4-(dimethylamino)pyridine (DMAP) in $CH_2Cl_2$. $^1$H NMR spectroscopy proved that ester formation had occurred (disappearance of the C$H_2$OH signal). By etching of the nanoparticles solution (in $CH_2Cl_2$) with an aqueous solution of $KI/I_2$ (0.02 M), followed by reduction of the excess of $I_2$ with $Na_2S_2O_3$, the gold core is transformed to an unidentified substrate, and the thiolates bound to gold are oxidized to disulfides and desorb.[26] The mass spectrum of the etching extract shows peaks at *m*/*z* values of 681.1 (oxidized phosphine/$CH_3$ mixed disulfide), 346.1 ($CH_3/CH_3$ symmetric disulfide), but not at 378.3, corresponding to the OH/$CH_3$ mixed disulfide, proving that all the hydroxyl groups had been converted into ester functionalities (within the accuracy of the mass spectrometer). Transmission electron microscopy (TEM) analysis provided an average size of the gold core of 2.0 ± 0.5 nm.

**Synthesis of Adsorbates and Dendrimer Wedges.** The synthesis of dendritic wedges **4** and **8** containing pyridine and phosphine ligands at their focal points, respectively, is outlined in Chart 2. Dendritic wedge **4** has hydrolyzable moieties at the periphery which can be used for further functionalization and growth of the molecule. The previously reported[16] adsorbate **9** (Chart 3) combines a dialkylsulfide moiety with an SCS $Pd^{II}$ pincer group and is therefore the anchoring molecule that is able to bind both to gold (via the sulfide) and to MPC **13** (Chart 3) and dendritic wedges **4** and **8** (via the $Pd^{II}$ pincer).

Adsorbates **11** and **12** (Chart 3) were synthesized in solution by removal of the inert chloride ligand of **9** with $AgBF_4$, followed by addition of dendritic wedges **4** and **8**, respectively. In the case of **4**, $^1$H NMR spectroscopy indicated that, in addition to the pyridine wedge, the sulfide also coordinated to $Pd^{II}$ because the binding strengths of the pyridine ester and the dialkylsulfide are similar. Two sets of signals were observed for both the pyridine α protons, the $CH_2S$ protons of the pincer system, and the $CH_2S$ protons of the sulfide moiety. Upon addition of excess pyridine wedge, an increasing amount of pyridine wedge coordinates to the $Pd^{II}$ pincer; however, a product free of coordinated sulfide could not be obtained.[27] Clearly, a ligand stronger than a pyridine ester is needed in order to avoid coordination of the sulfide to $Pd^{II}$. Therefore, we employed phosphine **8** as a ligand, which resulted in the quantitative formation of complex **12**. Previously, we have shown that phosphines are much stronger ligands for the SCS $Pd^{II}$ pincer system than pyridines.[28]

**Chart 2.** Synthesis of Dendritic Ligands **4** and **8**[a]

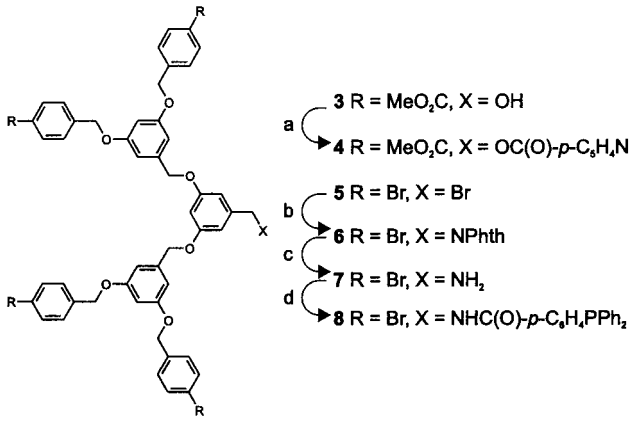


[a] (a) Isonicotinoyl chloride hydrochloride, $NEt_3$, $CH_2Cl_2$, rt, 8 H, 62%; (b) KNPhth, MeCN, reflux, 2 h, 85%; (c) $H_2NNH_2 \cdot H_2O$, EtOH, THF, reflux, 2 h, 90%; (d) 4-(diphenylphosphino)benzoic acid, DCC, HOBt, $CH_2Cl_2$, rt, 2 h, 85%.

**Chart 3.** Structure of Adsorbates **9**−**12** and Schematic Representation of Monolayer-Protected Au Nanocluster **13**

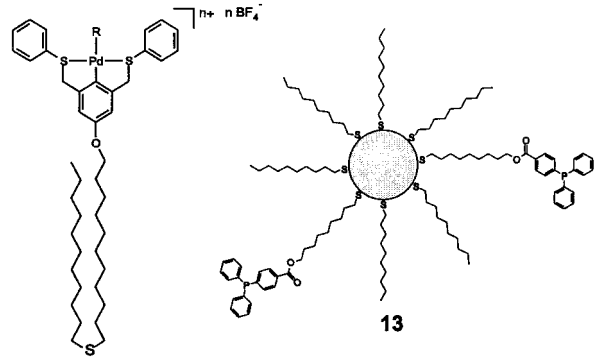


**9** R = $Cl^-$ (n = 0)
**10** R = pyridine (n = 1)
**11** R = **4** (n = 1)
**12** R = **8** (n = 1)

**Spatial Confinement of Au Nanoparticles on SAMs.** Monolayer experiments have been carried out using building blocks that are able to coordinate to SCS $Pd^{II}$ pincer moieties. The main reasons are the quantitative yield of the ligand

(25) Rubinstein, I.; Steinberg, S.; Tor, Y.; Shanzer, A.; Sagiv, J. *Nature* **1988**, *332*, 426−429.

(26) Templeton, A. C.; Hostetler, M. J.; Warmoth, E. K.; Chen, S.; Hartshorn, C. M.; Krishnamurthy, V. M.; Forbes, M. D. E.; Murray, R. W. *J. Am. Chem. Soc.* **1998**, *120*, 4845−4849.

(27) As a control experiment, 1 equiv of the pyridine wedge **2** was added to 1 equiv of a pincer system containing both a nonfunctional *n*-butyl chain instead of a sulfide chain and a labile acetonitrile ligand. Quantitative exchange of acetonitrile by the pyridine wedge was observed in this case, as evidenced by $^1$H NMR spectroscopy.

(28) van Manen, H.-J.; Nakashima, K.; Shinkai, S.; Kooijman, H.; Spek, A. L.; van Veggel, F. C. J. M.; Reinhoudt, D. N. *Eur. J. Inorg. Chem.* **2000**, 2533−2540.

exchange reactions involved[29] and the short reaction times required.[29,30]

Spatial confinement of Au nanoparticles on planar gold was achieved starting from isolated $Pd^{II}$ pincer adsorbate molecules **10** embedded into decanethiol SAMs on gold. The chloride of adsorbate **9** was first exchanged for a pyridine ligand in solution, and the resulting pincer molecules **10** were inserted into decanethiol SAMs by exposing the latter to a 1 mM dichloromethane solution of **10** for 3 h. This procedure avoids the use of $AgBF_4$ on a monolayer.[31] As expected, TM AFM images of these layers showed no features due to the small size of the $Pd^{II}$ pincer moiety protruding from the SAM. Subsequently, this substrate was immersed in a phosphine-functionalized colloid solution (0.4 mM in dichloromethane) for 10 min at r.t., followed by rinsing. Tapping mode AFM images acquired in air show the presence of nanosized features with a height of $3.5 \pm 0.7$ nm (Figure 1). This value correlates with the average nanoparticle size obtained by TEM, taking into account that the thickness of the alkyl chains can be measured by AFM, while TEM gives exclusively information about the metal core.[32] The particles do not form a complete monolayer, but are instead well separated and randomly distributed over the entire surface. This behavior is consistent with localized metal−ligand interactions between the phosphines of the Au nanoparticles and isolated $Pd^{II}$ moieties in the layer.

To rule out aspecific interactions or physisorption processes, sulfur-containing molecules with varying $\omega$-susbstituents were used to prepare monolayers both on flat gold and on the nanoparticles. Two different types of experiments were performed. In one case Au nanoparticles bearing only $CH_3$ and OH moieties as terminal groups were used and in the other the pincer sulfide **10** was not inserted into the decanethiol layer; all the samples were then imaged by TM AFM. The absence of adsorbed particles on these layers clearly supports the fact that both the phosphine moiety on the colloidal particles *and* the pincer molecules in the layers are necessary for the growth process, therefore the anchoring only occurs via metal−ligand interactions.

**Spatial Confinement of Dendrimers on SAMs: Optimization of Growth Conditions.** On the basis of the above-reported results, we anticipated the same process to occur using dendritic molecules. The growth of **11** and **12** on gold was carried out starting from isolated $Pd^{II}$ pincer adsorbate molecules **10** embedded into 11-mercapto-1-undecanol and decanethiol SAMs. These monolayers were subsequently exposed to 0.1 and 0.01 mM dichloromethane solutions of **4** and **8**, both for 10 and 60 min, and rinsed afterward with $CH_2Cl_2$ as described in the Experimental Section. In the case of the dendrimer wedge **4,** TM AFM images of the monolayer surface show only a few, very large features (8−9 nm in height), most likely physisorbed material. Similar images were obtained when a pure decanethiol SAM was immersed into a solution of **4** as a reference experiment. However, TM AFM images of monolayers that were exposed to dendrimer wedge **8** reveal the presence of isolated, nanometer-sized features (Figure 2). The different

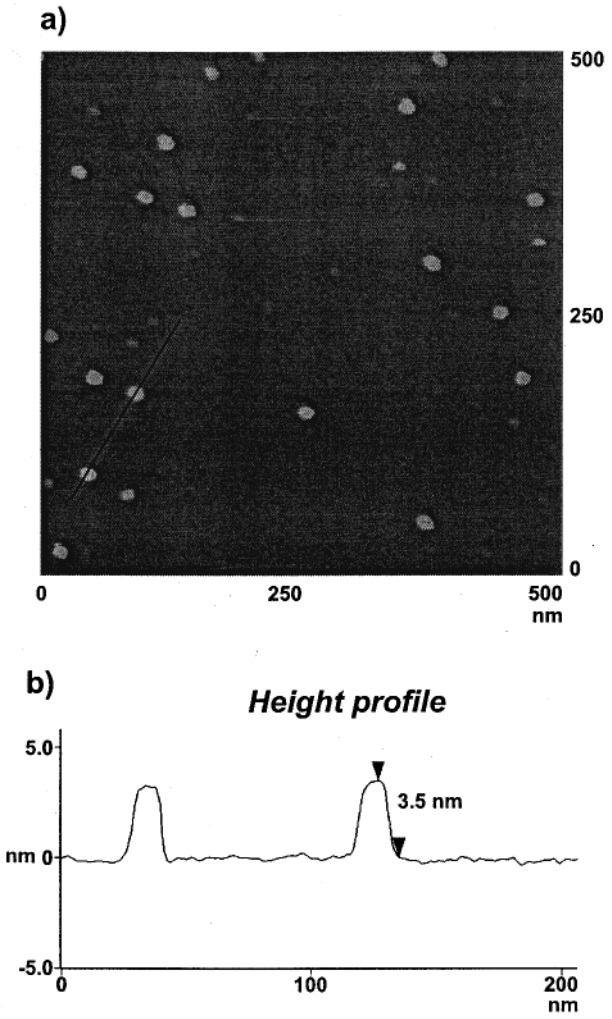


**Figure 1.** (a) TM AFM height image (acquired in air) of mixed monolayers of decanethiol and $Pd^{II}$ pincer sulfide **10** after exposure to a 0.04 mM dichloromethane solution of Au nanoparticle **13** for 10 min; (b) The height profile corresponds to the line drawn in the AFM image ($z$-scale = 10 nm).

reaction times (10 or 60 min) of the dendritic wedge **8** with the $Pd^{II}$ pincer-containing SAMs had no influence on the number of observed molecules.

The height and width of the isolated features, as determined by TM AFM in air, are $4.3 \pm 0.2$ nm and $15.3 \pm 4$ nm, respectively. The height of that part of the adsorbate which protrudes above the decanethiol monolayer, as obtained from a computer-generated model, is approximately 3.4 nm. Therefore, the average height, as determined by TM AFM, is in good agreement with the calculated value of the single molecules. The very soft tapping conditions employed in this experiment render the height value a good representation of the feature height.[33] The width of the dendrimer wedges appears to be much larger than in reality due to tip convolution.[34] The average number of nanometer-sized features counted in a $500 \times 500$ $nm^2$ area of the $Pd^{II}$ pincer-containing (**10**) decanethiol SAMs exposed to dendrimer wedge **8**, is $56 \pm 6$, which is in the same order of magnitude as we have previously found for direct insertion of other dendritic adsorbates.[16,17]

**Reference Experiments.** To certify that the nanometer-sized features observed in Figure 2 are single dendritic molecules,

(29) Huck, W. T. S.; van Veggel, F. C. J. M.; Reinhoudt, D. N. *Angew. Chem., Int. Ed. Engl.* **1996**, *35*, 1213−1215.

(30) (a) Huck, W. T. S.; van Veggel, F. C. J. M.; Kropman, B. L.; Blank, D. H. A.; Keim, E. G.; Smithers, M. M. A.; Reinhoudt, D. N. *J. Am. Chem. Soc.* **1995**, *117*, 8293−8294. (b) Huck, W. T. S.; van Veggel, F. C. J. M.; Reinhoudt, D. N. *J. Mater. Chem.* **1997**, *7*, 1213−1219.

(31) Deprotection with $AgBF_4$ of the coordinated chloride ligands of **9** inserted in a decanethiol monolayer gave rise to an insoluble residue (probably AgCl), which remained on the substrate, thereby hindering scanning force microscopy measurements.

(32) Reetz, M. T.; Helbig, W.; Quaiser, S. A.; Stimming, U.; Vogel, R. *Science* **1995**, *267*, 367−370.

(33) Brandsch, R.; Bar, G.; Whangbo, M.-H. *Langmuir* **1997**, *13*, 6349−6353.

(34) Schönherr, H. Ph.D. Thesis, University of Twente, The Netherlands, 1999.

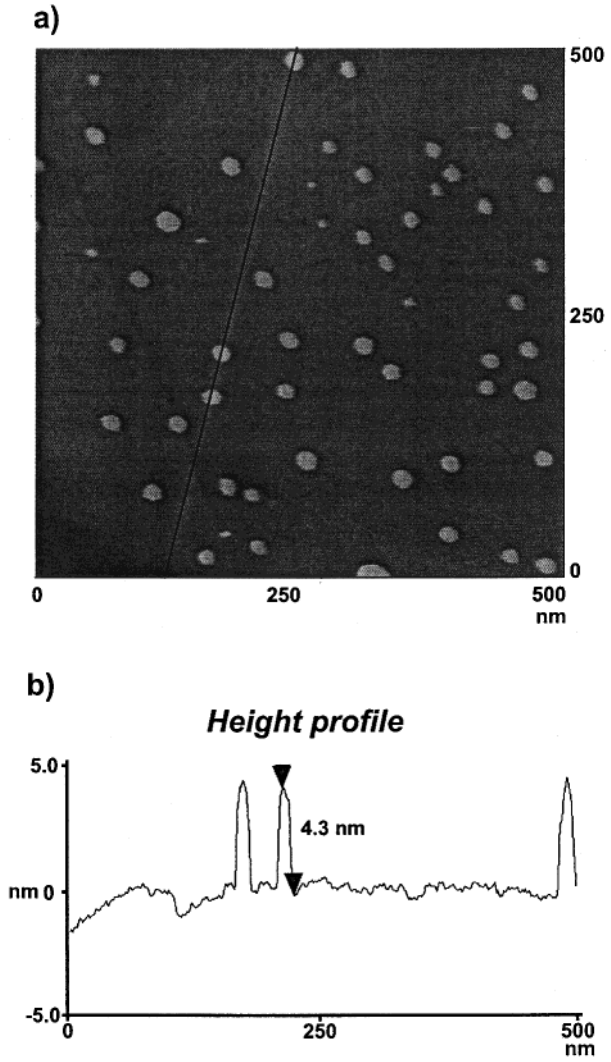


**Figure 2.** (a) TM AFM height image (acquired in air) of $Pd^{II}$ pincer-containing (**10**) decanethiol SAMs after exposure to a 0.01 mM dichloromethane solution of dendrimer wedge **8** for 10 min; (b) The height profile corresponds to the line drawn in the AFM image (*z*-scale = 10 nm).

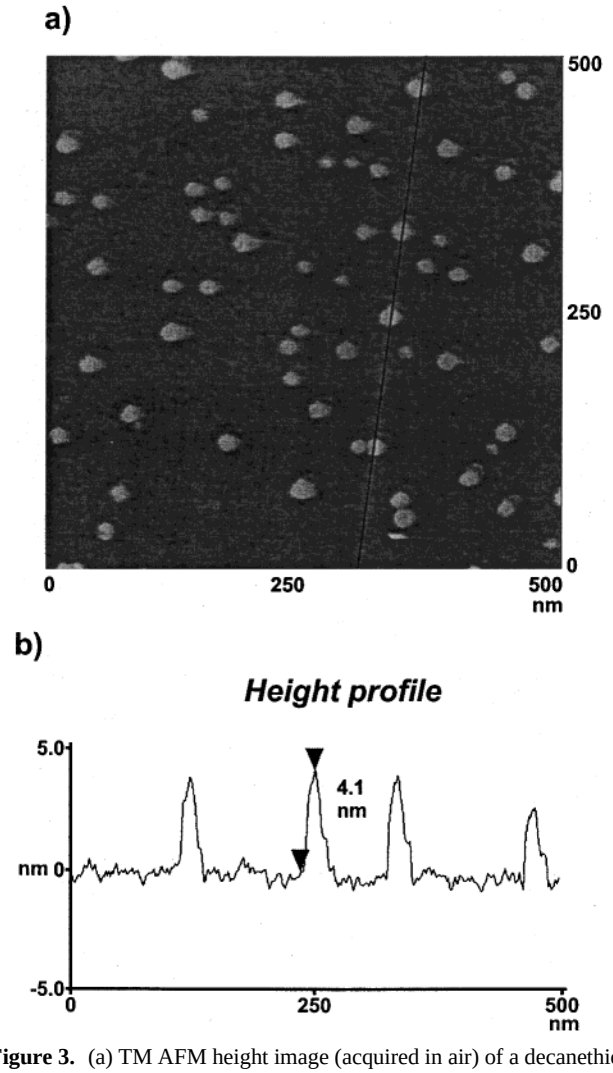


**Figure 3.** (a) TM AFM height image (acquired in air) of a decanethiol SAMs after exposure to a 1 mM dichloromethane solution of dendrimer adsorbate **12**, for 3 h; (b) The height profile corresponds to the line drawn in the AFM image (*z*-scale = 10 nm). The isolated dendrimer molecules appear slightly elongated due to a tip asymmetry.

direct insertion of dendritic adsorbate complex **12** was carried out, which should yield similar layers as the surface reaction described above. For this purpose, decanethiol SAMs were immersed in a 1 mM dichloromethane solution of **12**, for 3 h, and subjected to the same rinsing procedure as the layers which had been reacted with **8**. Using the same atomic force microscopy conditions as for the previous experiments, nanometer-sized features, very similar to those observed after the single-molecule growth experiments, were observed (Figure 3). The dendritic adsorbate molecules appear to be slightly elongated probably due to an asymmetry of the tip. The height and width of these features, as determined by TM AFM, are $4.1 \pm 0.2$ nm and $18.8 \pm 4$ nm, respectively, which correspond very well to the dimensions of the molecules synthesized on the monolayer by reaction of isolated $Pd^{II}$ pincer adsorbates, **10**, with dendritic wedge **8**.

In addition, the average number of nanometer-sized features counted in a $500 \times 500$ nm$^2$ area of the decanethiol monolayer exposed to a solution of dendrimer adsorbate **12**, is $51 \pm 9$. Again, this corresponds to the dendrimer coverage obtained by synthesizing the same dendritic adsorbate on the monolayer. These data strongly suggest that a significant number of the $Pd^{II}$ pincer adsorbates **10** inserted into the decanethiol monolayer, have reacted with the dendritic wedge molecules, **8**, forming a 1:1 complex in a similar way to the solution reaction. However, it should be taken into account that some $Pd^{II}$ pincer adsorbates might not be easily accessible to the dendritic wedge molecules in solution (e.g. if two or more $Pd^{II}$ pincer molecules adsorb close to each other in the SAM), thereby remaining in the monolayer, unreacted, and undetected. Further studies with larger molecules are currently being carried out to help clarify this matter.

Moreover, decanethiol SAMs devoid of $Pd^{II}$ pincer molecules were immersed in a 0.01 mM dichloromethane solution of **8** for 10 min. The absence of nanosized features on these layers confirmed that the isolated molecules shown in Figure 2 are not simply physisorbed to the SAM and that the $Pd^{II}$ center is indispensable for the attachment of the dendrimer wedges.

Insertion of adsorbate **10** into SAMs of 11-mercapto-1-undecanol was hampered by physisorption, as seen in TM AFM images. These TM AFM results were confirmed by contact angle measurements (with water) performed on the $Pd^{II}$ pincer-containing layers which had been exposed to 0.01 and 0.1 mM solutions of **8** (Table 1).

Various attempts to remove the physisorbed material using different rinsing procedures were made (see Experimental

**Table 1.** Advancing Contact Angles ($\theta_a$) and Hysteresis Values ($\Delta\theta$) of 11-Mercapto-1-undecanol Monolayers Containing $Pd^{II}$ Pincer Sulfide **10** after Exposure to 0.01 mM and 0.1 mM Solutions of **8**

| | 5 min $\theta_a/\Delta\theta$ (deg) | 30 min $\theta_a/\Delta\theta$ (deg) | 60 min $\theta_a/\Delta\theta$ (deg) |
|---|---|---|---|
| 0.01 mM | 36 ± 1/16 | 27 ± 1/13 | 27 ± 1/13 |
| 0.1 mM | 43 ± 1/29 | 41 ± 1/26 | 40 ± 1/26 |

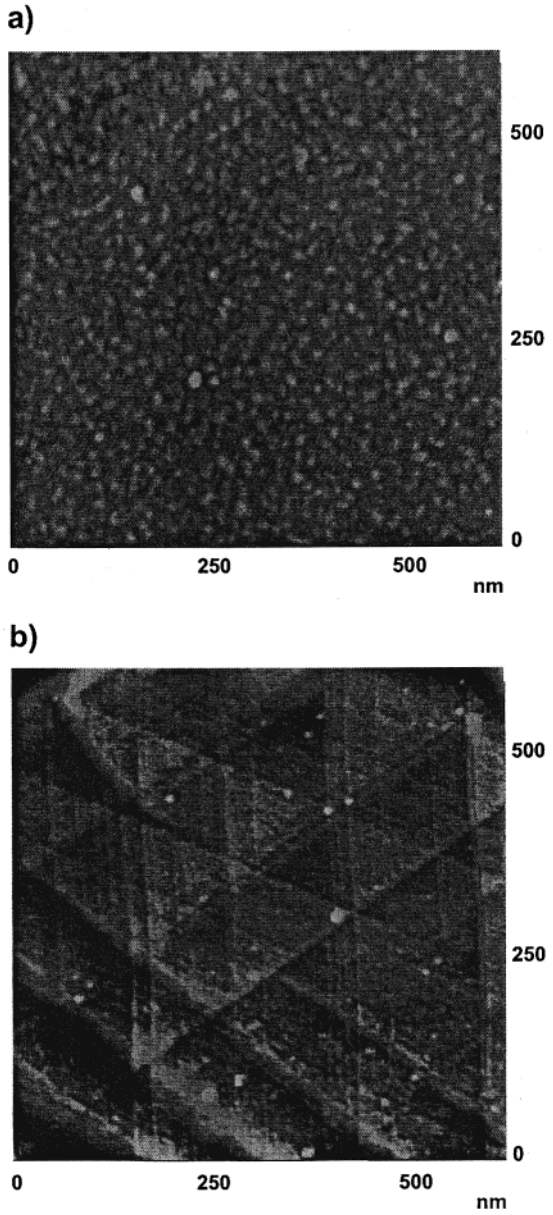


**Figure 4.** TM AFM height images of 11-mercapto-1-undecanol (a) and decanethiol (b) SAMs after immersion into a 0.1 mM dichloromethane solution of **8** for 1 h (*z*-scale = 5 nm). Both images were acquired in air.

Section), but they were not successful. AFM images of the alkyl-terminated SAMs show much less "contamination" than the corresponding hydroxyl-terminated surfaces, as can be seen from the results of the reference experiments carried out by immersing 11-mercapto-1-undecanol and decanethiol SAMs into 0.1 mM dichloromethane solutions of **8** for 1 h (Figure 4).

This shows that hydrogen bonding is the most probable cause of the physisorbed material observed on the 11-mercapto-1-undecanol SAMs. Some physisorbed material did remain on the decanethiol surface, most probably due to hydrophobic interactions between the layer and the dendritic wedges; however, this could successfully be removed by rinsing of the layer.

## Conclusions

Surface reactions on isolated molecules inserted into alkanethiol SAMs on gold have been performed. Coordination chemistry has been used to successfully grow isolated molecules into nanometer-sized adsorbates which can be detected by atomic force microscopy. This approach as a general strategy offers the possibility to isolate functional nanometer-sized objects, as shown by spatial confinement of different objects such as Au nanoparticles or dendritic structures on self-assembled monolayers. In principle it can be applied to any suitably designed nanosized object incorporating specific functions (e.g., semiconductor or magnetic nanoparticles). To render the "bottom-up" approach a viable option for the current "top-down" techniques in the manufacturing of nanometer-sized devices, two of the remaining challenges are currently being tackled: the exact positioning of nanometer-sized entities and the optimization of techniques able to detect and study such entities.

## Experimental Section

**General Procedures.** Melting points were determined with a Reichert melting point apparatus and are uncorrected. NMR spectra were recorded in $CDCl_3$ on a Varian Unity 300 locked to the deuterated solvent at 300.1 ($^1$H), 75.5 ($^{13}$C), and 121.5 ($^{31}$P) MHz, respectively. Chemical shifts are given relative to tetramethylsilane (TMS). FAB-MS spectra were recorded on a Finnigan MAT 90 spectrometer with *m*-nitrobenzyl alcohol (NBA) as the matrix. Elemental analyses were performed using a Carlo Erba EA1106. The presence of solvents in the analytical samples was confirmed by $^1$H NMR spectroscopy. Column chromatography was performed using silica gel ($SiO_2$, E. Merck, 0.040−0.063 mm, 230−240 mesh). Contact angle (CA) measurements were carried out on a KRÜSS Contact Angle Measuring System G10. Measurements for a drop of water whose volume was gradually increased (advancing CA) and then decreased (receding CA) were repeated on three sites of the same sample. For each receptor monolayer three samples were measured, and the average values are reported.

**Materials.** $CH_2Cl_2$ was freshly distilled from $CaCl_2$. Acetone, EtOH, THF, and $CHCl_3$ were used as received (p.a. from Merck). MeCN (p.a. from Merck) was stored over molecular sieves (4 Å). Water was purified by Millipore membrane units. Solvents for colloid preparation were of p.a. grade (from Merck). $HAuCl_4 \cdot xH_2O$ (99.99%, from Acros) and tetraoctylammonium bromide (from Fluka) were used as received. All other reagents and decanethiol were purchased from Aldrich and used without further purification. Dendritic wedges $Br_4$-[G-2]-Br (**5**)[35] and $(MeO_2C)_4$-[G-2]-OH (**3**),[36] and 11-mercapto-1-undecanol[37] were prepared according to literature procedures.

**$(MeO_2C)_4$-[G-2]-pyr (4)**. A solution of isonicotinoyl chloride hydrochloride (0.46 g, 2.6 mmol) and $NEt_3$ (0.85 mL, 6.1 mmol) in $CH_2Cl_2$ (25 mL) was added dropwise to a solution of dendritic wedge $(MeO_2C)_4$-[G-2]-OH (**3**) (1.00 g, 1.0 mmol) in $CH_2Cl_2$ (75 mL). The mixture was stirred at rt overnight under an argon atmosphere. After the addition of 1 M HCl (aqueous, 100 mL), the organic phase was separated and washed with $NaHCO_3$ (saturated) and brine and subsequently dried over anhydrous $Na_2SO_4$. After evaporation of the solvent in vacuo, the crude product was purified by column chromatography, using $CH_2Cl_2$/acetone 90:10 (v/v) as the eluent, affording a white solid. Yield 0.69 g (62%).

(35) Wooley, K. L.; Hawker, C. J.; Fréchet, J. M. J. *J. Chem. Soc., Perkin Trans. 1* **1991**, 1059−1076.
(36) Hawker, C. J.; Wooley, K. L.; Fréchet, J. M. J. *J. Chem. Soc., Perkin Trans. 1* **1993**, 1287−1297.
(37) Bain, C. D.; Troughton, E. B.; Tao, Y.-T.; Evall, J.; Whitesides, G. M.; Nuzzo, R. G. *J. Am. Chem. Soc.* **1989**, *111*, 321−335.

**$Br_4$-[G-2]-NPhth (6).** A mixture of dendritic bromide **5** (0.40 g, 0.36 mmol), potassium phthalimide (0.08 g, 0.43 mmol), and potassium carbonate (0.08 g, 0.58 mmol) in MeCN (50 mL) was refluxed under an argon atmosphere for 3 h. After evaporation of the solvent in vacuo, the resulting paste was taken up in $CH_2Cl_2$ (100 mL), and the solution was washed with brine and dried over $Na_2SO_4$. After removal of the solvent, the crude product was purified by column chromatography (eluent: $CH_2Cl_2$/hexane 80:20 (v/v)) to afford a white solid. Yield 0.41 g (96%).

**$Br_4$-[G-2]-$NH_2$ (7).** A solution of dendritic phthalimide **6** (0.14 g, 0.12 mmol) in EtOH (30 mL) and THF (10 mL) was heated to reflux, and hydrazine monohydrate (0.5 mL) was added. After refluxing for 2 h, the solution was cooled to room temperature and evaporated until 20 mL of solution remained. HCl (1 M, 50 mL) was added, and the solution was extracted with $CH_2Cl_2$ (2 × 50 mL). The organic layer was washed with $NaHCO_3$ (saturated) and brine and dried over $Na_2SO_4$. After evaporation of the solvent, the dendritic amine **7** was obtained as a colorless oil. Yield 0.12 g (96%). For characterization, the amine was further purified by column chromatography (eluent: $CH_2Cl_2$/MeOH 95:5 (v/v)).

**$Br_4$-[G-2]-phos (8).** To a solution of dendritic amine **7** (0.18 g, 0.17 mmol), 4-(diphenylphosphino)benzoic acid (48 mg, 0.16 mmol), and 1-hydroxybenzotriazole hydrate (HOBt, 21 mg, 0.16 mmol) in $CHCl_3$ (50 mL) was added 1,3-dicyclohexylcarbodiimide (DCC, 35 mg, 0.17 mmol). The mixture was stirred at room temperature under an argon atmosphere for 3 h. The solution was subsequently washed with $NaHCO_3$ (saturated) and brine and dried over $Na_2SO_4$. After evaporation of the solvent in vacuo the crude product was purified by column chromatography (eluent: $CH_2Cl_2$) to afford the dendritic phosphine wedge **8** as an off-white solid. Yield 0.18 g (79%).

**Sulfide Pincer, Pyridine Complex (10)**. To a solution of the sulfide pincer **9** (8.1 mg, 10.1 $\mu$mol) in $CH_2Cl_2$ (3 mL) were added a few drops of MeCN. Next, 78 $\mu$L (10.1 $\mu$mol) of a stock solution of $AgBF_4$ in water (0.130 M) was added, and the resulting mixture was stirred for 10 min. A white precipitate formed, indicating the formation of insoluble AgCl. Pyridine (90 $\mu$L of a 0.120 M stock solution in $CH_2Cl_2$, 10.8 $\mu$mol) was subsequently added. After stirring the mixture at rt for 10 min, the mixture was filtered through Hyflo into a 10 mL volumetric flask. The volumetric flask was filled with $CH_2Cl_2$ to 10 mL, providing a 1 mM solution of the pyridine complex of the sulfide pincer. For analytical investigation, this process was carried out in deuterated solvents.

**Sulfide Pincer, Pyridine Wedge Complex (11)**. The sulfide pincer **9** (4.1 mg, 5.1 $\mu$mol) was deprotected with $AgBF_4$ in the same manner as described above, and subsequently $(MeO_2C)_4$-[G-2]-pyr (5.5 mg, 5.1 $\mu$mol) was added. After filtration of the solution through Hyflo, the solvents were evaporated in vacuo. $^1$H NMR spectroscopy indicated coordination of both the pyridine wedge and the sulfide chain to $Pd^{II}$, for example $\delta$ (ppm) 8.8 and 8.4, respectively, for uncoordinated and coordinated $\alpha$-pyridyl protons.

**Sulfide Pincer, Phosphine Wedge Complex (12)**. The sulfide pincer **9** (4.3 mg, 5.3 $\mu$mol) was deprotected with $AgBF_4$ in the same manner as described above, and subsequently dendritic phosphine **8** (7.2 mg, 5.3 $\mu$mol) was added. After filtration of the solution through Hyflo, the solvents were evaporated in vacuo. This provided the product as a yellow solid in quantitative yield.

**Preparation of Mixed Monolayer-Protected Gold Colloids.** To a solution of tetraoctylammonium bromide (320 mg, 0.6 mmol) in toluene (6 mL) was added a solution of tetrachloroauric acid (200 mg, 0.6 mmol) in water (15 mL). $AuCl_4^-$ was transferred into the organic phase as witnessed by decoloration of the aqueous phase while the organic phase turned orange-brown. The mixture was stirred vigorously for 20 min to ensure complete transfer. Hereafter, a mixture of decanethiol (83.52 mg, 0.48 mmol) and 11-mercapto-1-undecanol (24.48 mg, 0.12 mmol) in toluene (15 mL) was added to the mixture. After 5 min, a freshly prepared aqueous solution (8 mL) of $NaBH_4$ (266 mg, 7.2 mmol) was added dropwise to the reaction mixture. The colloids were formed instantaneously as indicated by the color change of the solution from orange to red and then to black-brown. After 4 h, the organic layer was collected, washed with water, and dried over $Na_2SO_4$. The colloidal solution was then concentrated to 3 mL, and 300 mL of methanol were added to precipitate the colloids at −20 °C for 4 h. Centrifugation gave the colloids as a black solid (90 mg, 90% yield). They were repeatedly precipitated from methanol until there was no free ligand present. $^1$H NMR ($CDCl_3$, 300 MHz) $\delta$ 3.60 (bs), 1.47 (bs), 0.81 (bs).

**Etching of the Colloids.** Mixed monolayer-protected gold nanoparticles (20 mg) were dissolved in $CH_2Cl_2$ (20 mL) and then washed with a 0.1 M $I_2$/KI aqueous solution (2 × 30 mL). The excess of $I_2$ was removed by treating the solution with a $NaS_2O_3$ solution (2 × 30 mL) and washing with water. The solution was then dried over $Na_2SO_4$. By integration of the $^1$H NMR signals the amount of the two components in the MPCs was determined, and the percentage of the hydroxyl ligand was found to be 27%.

**Coupling Reaction on Mixed Monolayer-Protected Gold Colloids (13).** Mixed monolayer-protected gold colloids (15 mg) were dissolved in degassed $CH_2Cl_2$ (10 mL). To this solution was added 4-(diphenylphosphino)benzoic acid (0.75 mg, 0.24 $\mu$mol), EDC (0.68 mg, 3.5$\mu$mol), and DMAP (0.72 mg, 5.9 $\mu$mol), and the reaction mixture was stirred at room temperature for 2 h. The solution was concentrated to a minimum amount (0.5 mL), and 300 mL of degassed methanol was added to precipitate the colloids at −20 °C for 4 h. After centrifugation and washing with methanol, a quantitative yield of the colloids was obtained. $^1$H NMR showed broad spectra, and no signal was observed from $^{31}$P NMR spectroscopy. The colloids were then etched by $I_2$/KI in a similar procedure as described above. The organic residue was analyzed by FAB mass spectroscopy. Found: *m*/*z*: 681.1 ($[M + H]^+$; calcd for $C_{40}H_{57}O_3PS_2$: 680.3), 346.1 ($[M]^+$, calcd for $C_{20}H_{42}S_2$: 346.3).

**Substrate Preparation.** Gold substrates were obtained from Metallhandel Schröer GmbH (Lienen, Germany). Immediately before use, the substrates were rinsed with high-purity water (Millipore) and then flame-annealed with a $H_2$ flame (purity 6) as described previously.[38] After the annealing procedure, the substrates were placed in p.a. ethanol for 10 min[39] and then immersed into the adsorbate solution for the desired time. All adsorbate solutions were prepared just before use. After each adsorption step the samples were removed from the solutions and rinsed thoroughly with dichloromethane, ethanol, and water (Millipore). SAMs of 11-mercapto-1-undecanol and decanethiol were prepared by immersing the gold substrates in the corresponding 1 mM ethanol solutions at room temperature for 3 h. Solutions of **8**, **12**, and **13** were deoxygenated prior to immersion of the monolayers by bubbling $N_2$ through the solutions for 10 min and were kept under Ar during the monolayer experiments. After immersion into solutions of **4**, **8**, **11**, **12**, or **13**, the samples were rinsed by placing them in $CH_2Cl_2$ for 3 × 5 min (3 × 20 mL $CH_2Cl_2$). Two other rinsing procedures were attempted: (a) $CH_2Cl_2$ (20 mL, 5 min), followed by EtOH (20 mL, 5 min) and $H_2O$ (20 mL, 5 min), and (b) 15 min in $CH_2Cl_2$ in the sonicator, but some physisorbed material remained on the layers. Hydrophilic layers were dried under a nitrogen stream. All experiments were repeated 3−4 times.

**Atomic Force Microscopy**. The AFM measurements were carried out with a NanoScope III multimode AFM (Digital Instruments, Santa Barbara, CA). Tapping mode AFM scans were performed in air using silicon cantilevers/tips (Nanosensors, Wetzlar, Germany; cantilever resonance frequency $f_0$ = 280−320 kHz). The free amplitude was kept constant for all experiments, and the amplitude damping (setpoint) ratio was adjusted to ˜0.90. Prior to the measurements the setup was thermally equilibrated for several hours to minimize the drift and to ensure a constant temperature (˜30 °C). The piezo scanner was calibrated in lateral directions using a grid with repeat distances of 1.0 $\mu$m, as well as self-assembled monolayers of thiols on Au(111) (e.g. octadecanethiol, repeat distance 0.51 nm),[38] and in *z*-direction by measuring step heights of Au(111) (2.9 Å). The number of nanometer-sized features and their standard deviations were determined by counting the features on at least four areas of the same sample, and taking the average.

(38) Schönherr, H.; Vancso, G. J.; Huisman, B.-H.; van Veggel, F. C. J. M.; Reinhoudt, D. N. *Langmuir* **1999**, *15*, 5541−5546.
(39) Ron, H.; Rubinstein, I. *Langmuir* **1994**, *10*, 4566−4573.

**Acknowledgment.** Financial support of this research by the Council for the Chemical Sciences of The Netherlands Organization for Scientific Research (CW-NWO) is gratefully acknowledged.

**Supporting Information Available:** Characterization of compounds **4**, **6**, **7**, **8**, **10**, and **12** by melting point, $^{1}H$, $^{13}C$, and $^{31}P$ NMR spectroscopy, FAB mass spectrometry, and elemental analysis (PDF). This material is available free of charge via the Internet at http://pubs.acs.org.

JA010257C